Evaluation of experimental procedures for confined concrete columns using 3D finite element analyses

H. O. Köksal[1], C. Karakoç[2], Z. Polat[1], T. Turgay[1] & Ş. Akgün[1]
[1]*Civil Engineering Faculty, Yıldız Technical University, Turkey*
[2]*Civil Engineering Department, Boğaziçi University, Turkey*

Abstract

This paper presents the results of the early stages of both a continuing experimental work on the square confined concrete columns and their 3D finite element modeling based on the isotropic damage theory in order to establish a realistic approach for the confinement pressure. Based on the axial behavior of four RC columns with a 200 mm square cross section tested under concentric loading, existing experimental data and procedures in the literature are evaluated. As demonstrated from the comparison of the FE analysis and the test results, obtaining a uniform axial loading and deformation state is questionable.
Keywords: confinement pressure, reinforced concrete column, finite element, isotropic damage theory, geometrical defects.

1 Introduction

The compressive strength of RC columns increase with increasing confining pressure. The confinement mechanisms are transverse reinforcements such as stirrups or spirals, FRP wraps, and steel jackets, etc. extensive research on the axial behavior of confined concrete has been carried out since the pioneering study of Richardt et al. [1].

The constitutive model for confined concrete based on the experimental findings plays an important role in the pushover analysis of RC structures. There are some frequently cited models (Hognestad [2], Kent and Park [3], Sheikh and Uzumeri [4], Mander et al. [5], Saatcioglu and Razvi [6]) to predict the peak stress or the stress–strain curve of confined concrete. Only the latest two

WIT Transactions on Modelling and Simulation, Vol 46, © 2007 WIT Press
www.witpress.com, ISSN 1743-355X (on-line)
doi:10.2495/CMEM070251

recommends a relation for finding the confining pressure. Mainly two experimental works conducted by Sheikh and Uzumeri [7], Mander et al. [8], are employed mainly for derivation of these relations.

Techniques for measuring longitudinal deformations and the effects of possible small defects on the cross-section of the columns during the production of the specimens to the experimental results are evaluated.

2 Experimental work

The square specimens in the test program have 200x200 mm cross-section dimensions and 1000 mm height. The columns tested in the structural laboratory of Yıldız Technical University, are a first part of a Ph.D. study about confined RC columns. Fig. 1 shows the details of test setup and instrumentation.

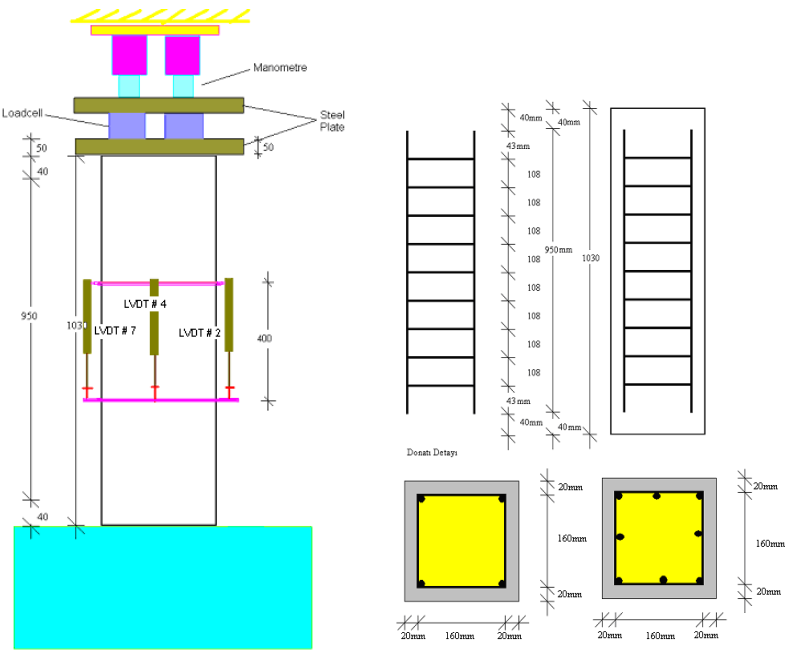

Figure 1: Test setup and the details of test specimens.

There is only one type of concrete mix for all test columns. C1, C2, and C3 type columns are tested respectively at 30 days, 60 days and 90 days. All longitudinal bars are 10mm in diameter and L4 and L8 shows the number of the bars in the cross-section of a column. The tie spacing is 100mm and the S8 and S12 represent tie diameters. In this paper, the results of the C1 type-columns are presented.

For measurement of axial strains, four linear variable displacement transducers (LVDTs) are placed over the central 400mm gage length at each side of a column in a similar way used to assess any eccentricity of the applied load

as recommended in the study of Shrive et al. [9]. A pre-loading up to the one-fourth of the predicted axial capacity is applied to maintain similar displacement readings at LVDTs so that in the linear elastic stage of the overall behavior any eccentricity can be eliminated.

Similar procedures have been used for measuring the axial shortening in the literature. In the experimental study of Sheikh and Uzumeri [7], the load versus deformation behavior of the test region of the columns was recorded using two linear variable displacement transducers (LVDT), one on the west, and the other on the east side of the column. Strain curves were averaged along the strain axis to obtain the mean load versus average strain characteristics of the test region. Mander et al. [8] took several readings of longitudinal strains over the central 450mm gage length of each column using four linear potentiometers. The average of the four potentiometers around the circumference was used prior to reaching maximum load. After this load level, some critical potentiometers were defined by establishing that the failure region occurred wholly within the gage length of the potentiometers instead of averaging the readings of four potentiometers.

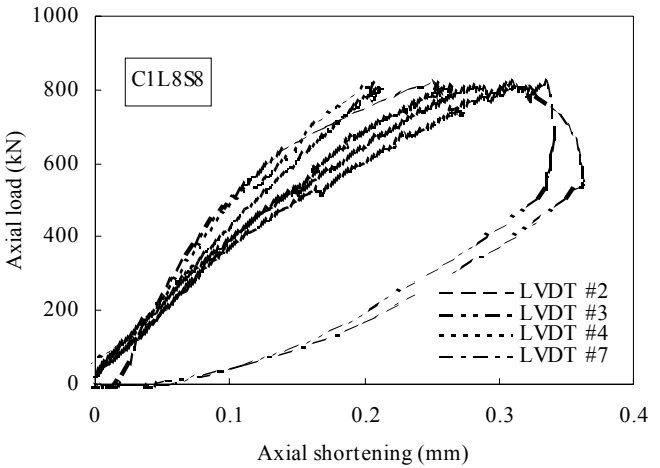

Figure 2: Four separate LVDT readings of axial load-shortening curves for the column specimen C1L8S8.

Although the LVDT readings were provided very close to each other, next to the maximum axial load there can be a significant variation between the minimum and maximum values of shortening reaching very high values.

3 3D Finite element modeling of RC columns

The concrete elements are modeled using eight-noded isoparametric solid continuum elements. Vertical and lateral reinforcements are meshed using two-noded 3D bar elements. Taking the advantage of symmetry and uniform loading

of system, 3D model of the concentrically loaded RC columns is created using one-fourth of the cross-sectional symmetry. The bottom surface is fully restrained while the lateral translations are only restricted in the top surface [10].

The Oliver's damage model [11] primarily developed for concrete elements and now available within the LUSAS software package [12], are employed for the material modeling of concrete. There are initially three parameters, which have to be defined before the analysis:

1) The initial threshold, τ^*, can be given as

$$\tau^* = \frac{f_t}{\sqrt{E_0}} \tag{1}$$

CEB-FIB [13] Equation is adopted for the initial elasticity modulus of elasticity, E_0:

$$E = \alpha * 21500 * \left(\frac{f_c}{10}\right)^{1/3} \tag{2}$$

in which f_c is the cylindrical compressive strength of concrete at 28 days. f_t is taken as

$$f_t = 0.35\sqrt{f_c} \tag{3}$$

2) A material parameter, A, is a limiting factor of the maximum size of the element that used for a mesh size choice and is given by [11]

$$A = \left(\frac{G_f E_0}{h f_t^2} - \frac{1}{2}\right) \geq 0 \tag{4}$$

in which h is the characteristic length of the finite element and G_f is the fracture energy of concrete. A simple analytical relation, derived from a semi-theoretical approach [14] is used for the fracture energy of concrete:

$$G_f = 15.5\, d_{\max} \frac{f_t^2}{E_0} \tag{5}$$

in which d_{max} is the maximum aggregate size in the concrete mix. A final form of A can be obtained as in a previous study [15]

$$A = \frac{h}{310} \tag{6}$$

Eq (6) clearly reflects only the mesh size effect into the analysis. A representative mesh size for nonlinear FEA can be used in this study as recommended by Bazant and Oh [16]:

$$h = \sqrt[3]{h_x\, h_y\, h_z} \tag{7}$$

where h_x, h_y, and h_z are sizes of an eight-noded solid element.

An ideal elasto-plastic behavior is adopted with a Von Misses type of stress potential for steel elements. 3D-bar elements are used for the reinforcing steel bars and ties.

3) A damage ratio is the ratio of the stresses that cause initial damage in tension and compression.

4 Model verification and evaluation of experimental results

3D-Finite element analyses of four RC columns tested in the structural laboratory of Yıldız Technical University are performed in this study. As shown in fig.3 and fig.4, the mesh sizes chosen for concrete elements are optimum sizes since the expression for material parameter A in eq (6) is derived for representative concrete meshes having approximately a size of three times the maximum aggregate diameter [16–18].

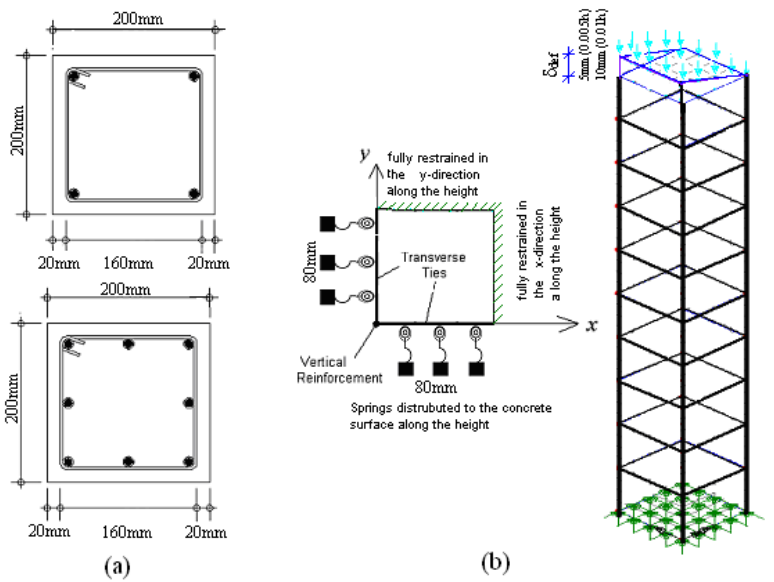

Figure 3: (a) Cross-sectional dimensions and (b) FE meshing of RC columns with and without any defects.

Figure 4: (a) Test setup; (b) Failure of a RC column.

It is important to model the confining action of the stirrups properly. If only the bar elements are used for ties, there is no possibility to reflect the confining action of ties between two nodes. Therefore, springs, acting on the lateral surface of concrete element are defined and the total spring stiffness acts on the nodes as shown in fig.3.

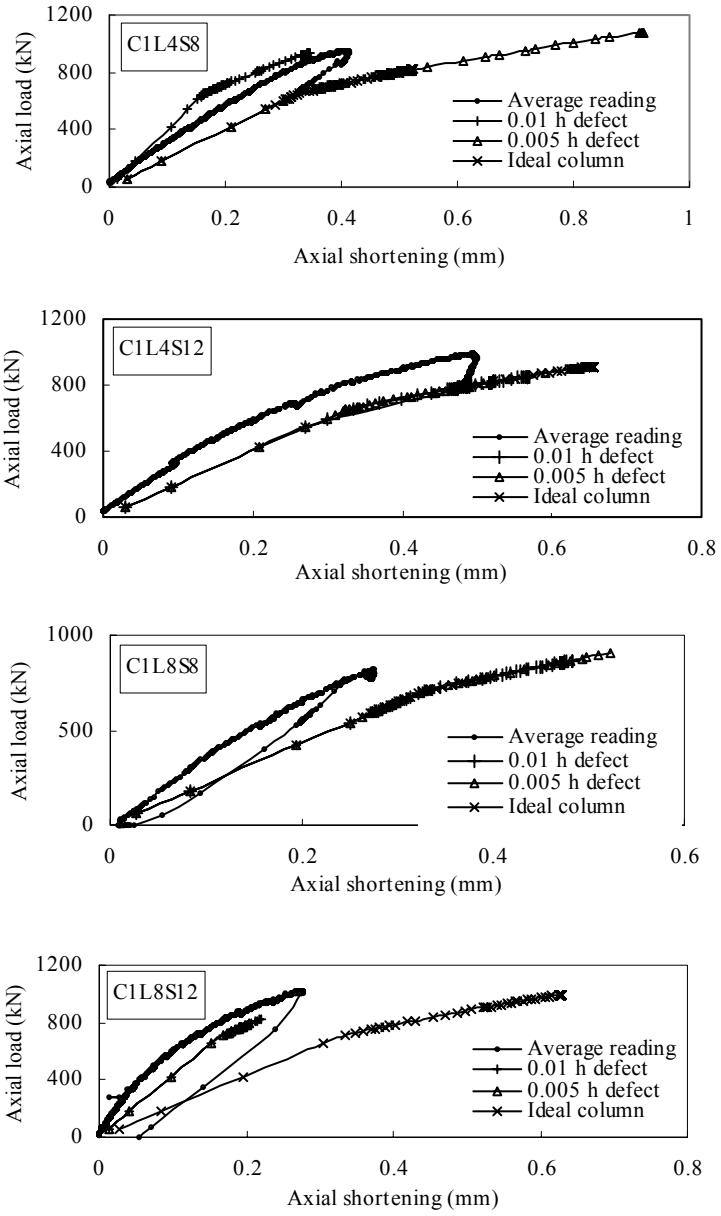

Figure 5: Influence of geometrical defects on axial load-shortening curves of finite element analysis and comparison with the experimental results obtained from averaging the readings of three LVDT's.

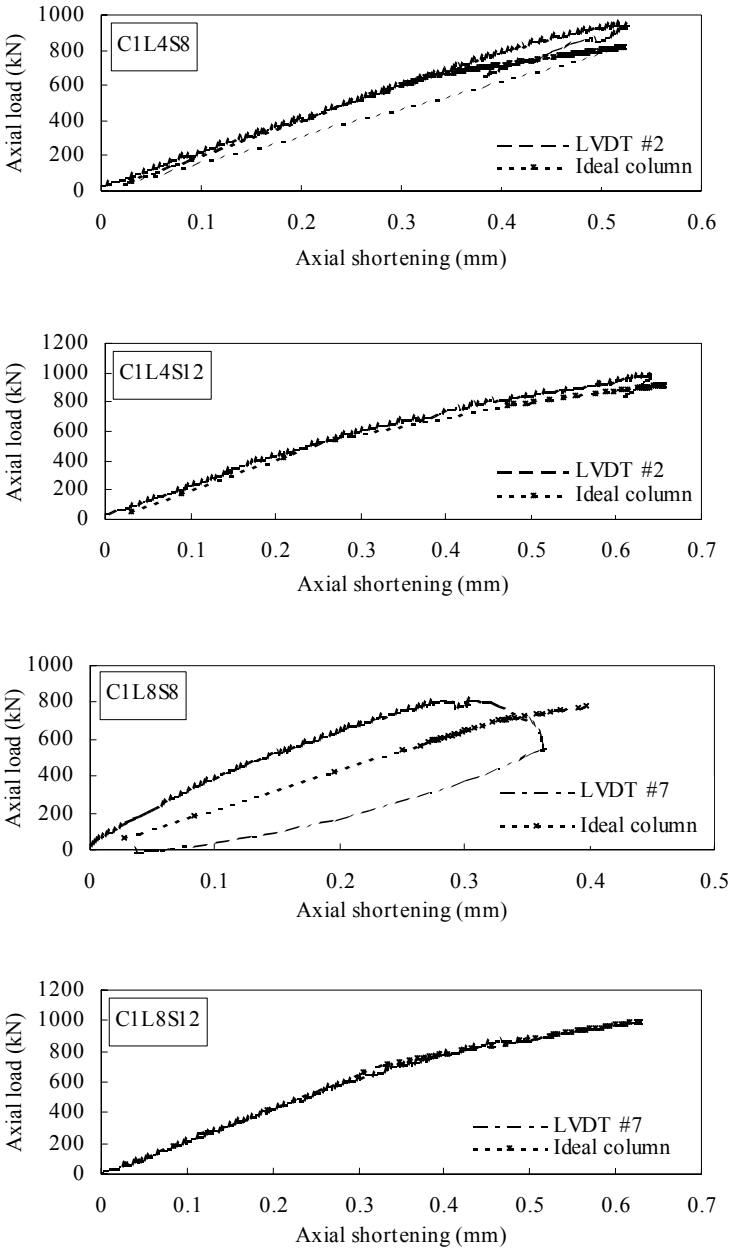

Figure 6: Comparison of the readings of the critical LVDT located on the heavily damaged region and the results of FEA of an ideal column.

The assumption of existing of some specific geometrical defects is initially imposed on the cross-section of the column as shown in fig. 3(b). A perfect flat top surface is modified to a deformed one by imposing a height difference of 10mm (0.01h) and 5mm (0.005h) respectively to one edge of the column. These deformations are really small values, which cannot be observed easily. As can be seen in fig.5, the results obtained from finite element analysis of deformed specimens for the axial load-shortening curves get closer to the curve drawn averaging readings of three LVDTs.

It is clearly stated that there is no ideal column subjected to a perfect concentric loading up to the failure load. Especially, when the plastic deformations are getting larger at approximately 75% of the maximum load, the cracks begin to grow unstably and macro-cracks arise pointing out the localization of the damage. The readings obtained from the critical LVDT and shown in fig.6 are also close to the results of the 3D finite element analysis of an ideal RC column. The critical LVDT represents the readings belonging to the heavily deformed side of the column, even the differential settlement of this side due to the localized damage can be observed by naked eye. While the test column continues to consolidate near to the failure load, volumetric expansion occurs by the opening of macro cracks on the adjacent side of the column as shown in fig.7. A similar approach is adopted by Mander et al. [8] defining some critical potentiometers on the failure region within the gage length of the potentiometers instead of averaging the readings of four potentiometers. However, it is clear that there is an uncertainty about the exact place of the localized damage region on which the critical LVDT to be placed for obtaining the maximum shortening values of the column.

Figure 7: (a) Heavily consolidated side; (b) macro-crack at neighbouring side.

5 Conclusion

This paper has been concerned with the evaluation of the experimental techniques for obtaining the axial load-shortening curves of RC columns subjected to concentric loading. Comparing the experimental data and 3D finite element analyses of four RC columns tested in the structural laboratory of Yıldız Technical University, some uncertainties measuring the axial deformation is studied.

For this purpose, while the average of LVDTs can be used near to the failure load, the critical LVDT readings showing the accumulated damage on heavily consolidated side of the column should be preferred after the beginning of the unstable crack propagation approximately taken as 75% of the failure load. The FEA results and experimental data show good agreement for this case. On the other hand, there is some uncertainty about the exact place for the replacement of the critical LVDT on the failure region. Alternative places for the LVDT on this damaged side of the column may be schemed for measuring the consolidation of the column. Thus, a need for a definition for the replacement of the critical LVDT to measure the axial deformations of RC columns is apparent. Even it is possible to use some averaging values for the determination of the axial shortening.

If a very small height difference between two opposite sides on the top surface of the specimen is imposed on the 3D modelling of columns, the results of FEA and the average of LVDTs are close to each other. This kind of defects is possible during the preparation stage of the specimens and should be carefully checked.

Acknowledgement

The support of B.U. Research Fund (ref: research project 05A403) for this paper is gratefully acknowledged.

References

[1] Richart, F.E., Bradtzaeg, A. & Brown, R. L., *A study of the Failure of Concrete under Combined Compressive Stresses*, Bulletin Np. 185, Engineering experimental station University of Illinois, Urbana, pp. 104, 1928.

[2] Hognestad, E., *A Study of Combined Bending and Axial Load in Reinforced Concrete Members*, Bulletin Series No.399, University of Illinois Eng. Exp. Station, Urbana. 1951.

[3] Kent, D.C. & Park, R., *Flexural Members with Confined Concrete*, Journal of the Structural Division, Proc. of the American Society of Civil Engineers, 97(ST7), pp.1969-1990, 1971.

[4] Sheikh, S.A. & Uzumeri, S.M., *Analytical Model for Concrete Confinement in Tied Columns*, Journal of the Structural Division, Proc. of

the American Society of Civil Engineers, 108(ST12), pp. 2703-2722, 1982.

[5] Mander, J.B., Priestly, M.J.N. & Park, R., *Theoretical Stress-Strain Model for Confined Concrete*, Journal of the Structural Engineering, ASCE, 114(8), pp.1804-1826, 1988.

[6] Saatcioglu, M. & Razvi, S.R., *Strength and Ductility of Confined Concrete*, Journal of the Structural Engineering, ASCE, 118(6), pp.1590-1607, 1992.

[7] Sheikh, S.A. & Uzumeri, S.M., *Strength and Ductility of Tied Concrete Columns*, Journal of the Structural Division, ASCE, 106(ST5), pp.1079-1102, 1980.

[8] Mander, J.B., Priestly, M.J.N. & Park, R., *Observed Stress-Strain Behavior of Confined Concrete*, Journal of the Structural Engineering, ASCE, 114(8), pp.1827-1849, 1988.

[9] Shrive, P.L., Azarnejad, A., Tadros, G., McWhinnie, C. & Shrive, N.G, Strength *of Concrete Columns with Carbon Fibre Reinforcement Wrap*, Canadian Journal of Civil Engineering, Volume 30, pp. 543-554, 2003.

[10] Karakoç, C., Köksal, H.O., & Özsoy, A.E., *The Behaviour of Reinforced Block Masonry Columns Under Axial Compression,* Earthquake Resistant Engineering Structures IV, WIT Press, Southampton, U.K., pp. 371-379, 2003.

[11] Oliver, J., Cervera, M., Oller, S. & Lubliner, J., *Isotropic Damage Models and Smeared Crack Analysis of Concrete*, In N. Bićanić et al. (ed) Proc. SCI-C Computer Aided Analysis and Design of Concrete Structures, pp. 945-957, 1990.

[12] LUSAS Modeller (v13.6) User Manual v13, FEA ltd., UK

[13] CEB-FIB. 1990 Model Code. Comité Euro-International du Béton (CEB), Lausanne, Switzerland.

[14] Köksal, H.O., *Modelling of Concrete Fracture*, Ph.D. thesis, Division of Civil Engineering, Boğaziçi University, İstanbul, Turkey, 1998.

[15] Köksal, H.O., Doran, B., Özsoy, A.E. & Alacali, S.N., *Nonlinear Modeling of Concentrically Loaded Reinforced Blockwork Masonry Columns,* Canadian Journal of Civil Engineering, Volume 31, Number 6, pp.1012-1023, 2004.

[16] Bažant, Z.P. & Oh, B., *Crack Band Theory for Fracture of Concrete*, Materiaux et Constructions, 16, 93, pp.155-177, 1983.

[17] Bedard, C. & Kostovos, M.D., *Fracture Process of Concrete for NLFEA Methods*, ASCE Journal of Structural Engineering, 112, 3, 573-586, 1986.

[18] Köksal, H.O. & Arslan, G., *Damage Analysis of RC Beams without Web Reinforcement,* Magazine of Concrete Research, Volume: 56, pp.231-241, 2004.